

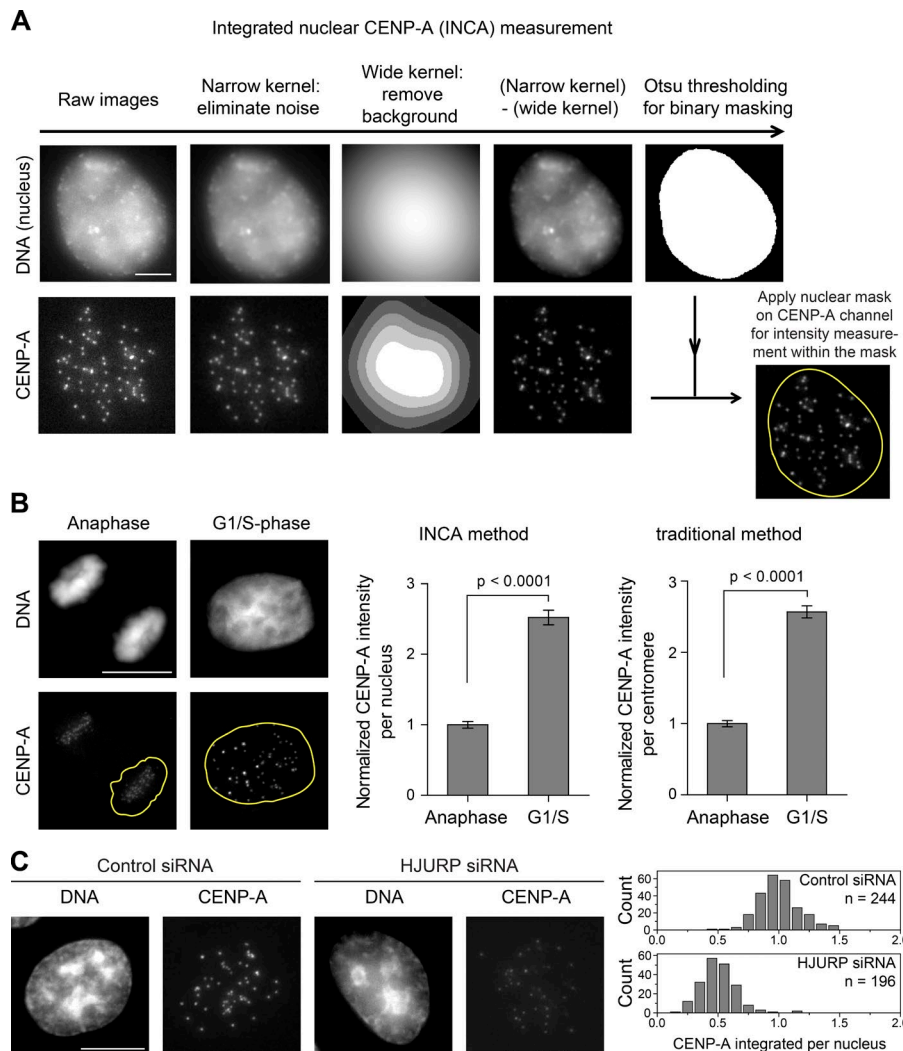
Liu and Mao, <http://www.jcb.org/cgi/content/full/jcb.201512034/DC1>

Figure S1. **The integrated nuclear CENP-A (INCA) measurement.** (A) Automatic routine of the INCA method based on a previous study (Lagana et al., 2010) with minor modifications. See Materials and methods for more details. Bar, 5 μ m. (B) A proof-of-principle application of the INCA method showing consistent conclusions with the traditional method when comparing centromeric CENP-A levels between anaphase and G1/S phase cells (representative images with nuclear masks outlined in yellow). Quantification of the normalized CENP-A integrated intensity following the INCA method (means \pm 95% confidence intervals). Anaphase: $n = 156$; and G1/S: $n = 138$ cells from three independent experiments. CENP-A levels are approximately doubled in G1/S compared with anaphase. This result is consistent with the quantification using the traditional method (means \pm 95% confidence intervals). Anaphase daughter cells: $n = 423$; and G1/S cells: $n = 529$ single centromeres randomly measured from the same cells used in the INCA measurement. Bar, 10 μ m. The p-value was computed using a two-tailed t test. (C) Another proof-of-principle application of the INCA method showing reduced CENP-A levels in cells depleted of HJURP. Histograms showing normalized CENP-A integrated intensity plotted from control ($n = 244$) and HJURP siRNA ($n = 196$) cells (from three independent experiments and $P < 0.0001$ by two-tailed t test). Bar, 10 μ m.

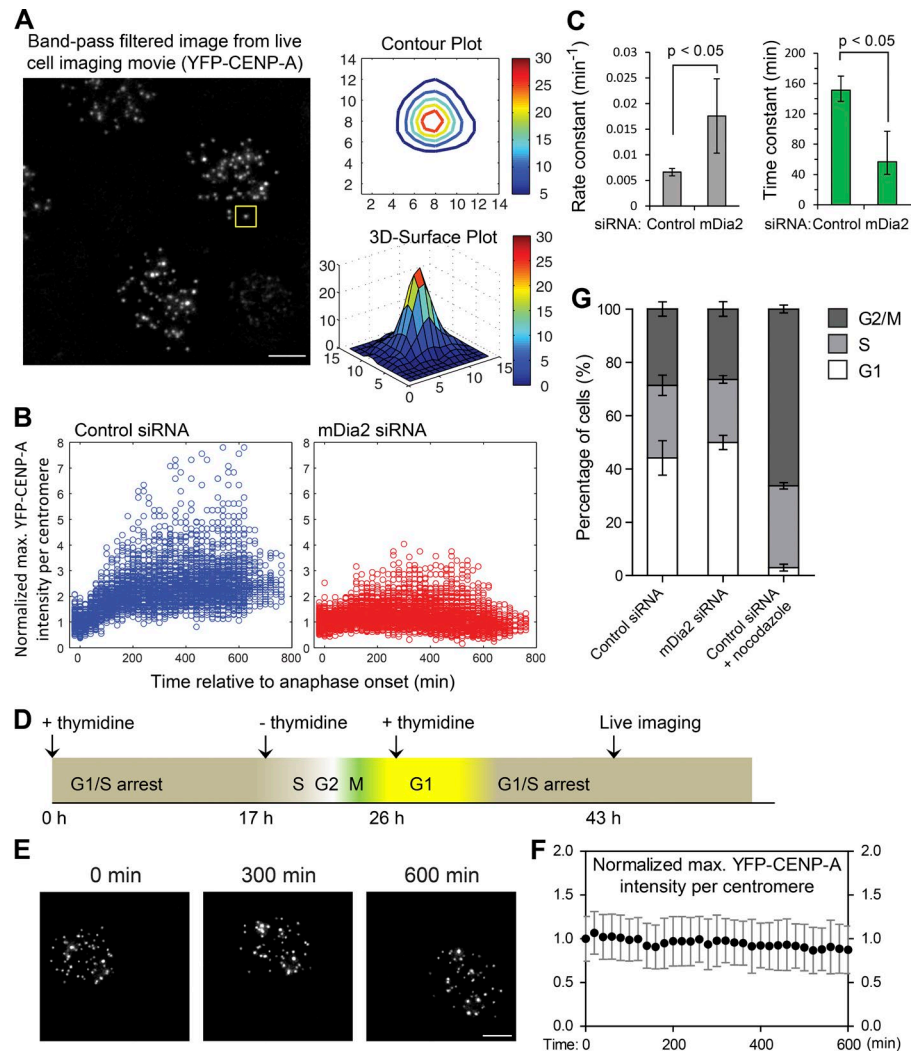


Figure S2. **The method used for quantifying high-resolution ratiometric live-cell imaging data and details of nonlinear regression.** (A) YFP-CENP-A signals approximately follow Gaussian distribution at centromeres, making it reasonable to use local maxima for the measurement of centromeric CENP-A levels. Bar, 5 μm . (B) Raw scatterplots of ratiometric CENP-A levels on individual centromeres, which were used for plotting mean \pm SD for control cells and mDia2 siRNA-treated cells in Fig. 2 B. (C) Bar graphs comparing the “apparent” rate constant and time constant between control cells and mDia2 siRNA-treated cells. Apparent rate and time constants were computed from nonlinear regression using one phase association model. In total, $n = 4,100$ centromeres from 12 G1 pairs for control and $n = 4,310$ centromeres from 13 G1-pairs for mDia2 siRNA cells were analyzed and plotted (means \pm 95% confidence intervals). (D) Scheme of thymidine synchronization and live imaging of G1/S cells with fully loaded CENP-A levels. This was designed to test for photobleaching over long-term live-cell imaging. (E) Representative frames from live imaging movie of YFP-CENP-A in arrested G1/S cells (Video 3). Imaging setup was identical to that used in Fig. 2, and images were scaled on the same dynamic range over time. Bar, 5 μm . (F) Quantification of centromeric YFP-CENP-A levels over time (plotted as mean \pm SD). For every time point, 100 centromeres in 10 cells were measured from two repeated experiments (See Materials and methods for more details). (G) Depletion of mDia2 does not affect cell cycle. Quantification of the percentage of cells within each cell cycle stage (mean \pm SD; $n = 30,000$ cells per treatment from three independent experiments). The univariate model was used for FACS data analysis (Watson et al., 1987). The p-value was computed using a two-tailed t test. G1 control versus mDia2 siRNA, $P = 0.2254$; G1 control versus control + nocodazole, $P = 0.0004$; S control versus mDia2 siRNA, $P = 0.2007$; S control versus control + nocodazole, $P = 0.2031$; G2/M control versus mDia2 siRNA, $P = 0.3782$; G2/M control versus control + nocodazole, $P < 0.0001$.

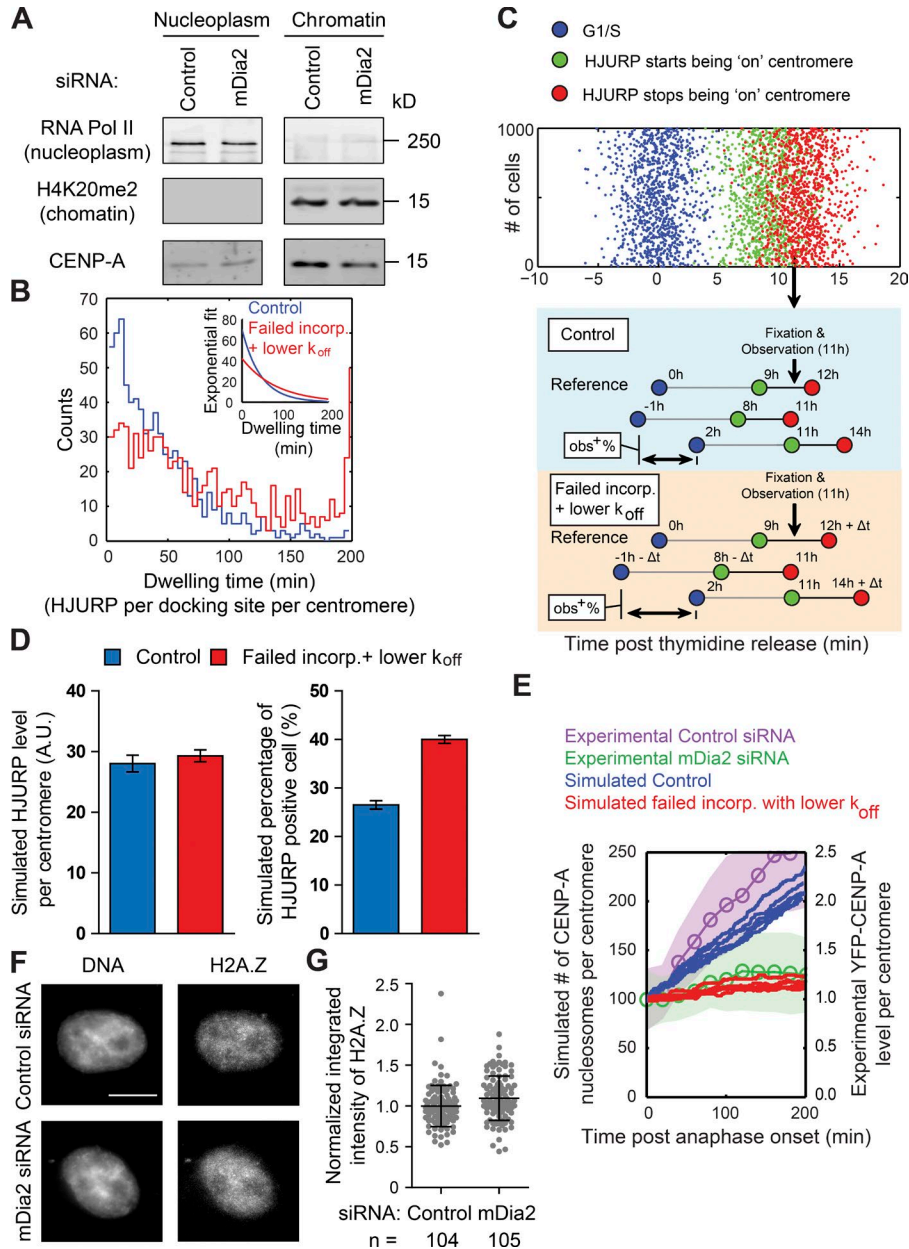
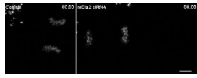
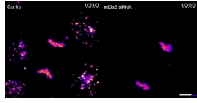


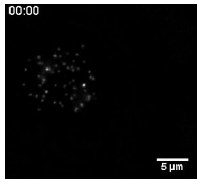
Figure S3. **Stochastic simulation of HJURP turnover at G1 centromeres.** (A) Pairwise immunoblots showing relative levels of nucleoplasmic and chromatin-bound CENP-A proteins in control cells and cells depleted of mDia2. (B) Histograms of the distribution of single dwelling events per docking site per centromere. Exponential fits were given as inset. For control and perturbed conditions, $n = 761$ and $n = 855$, respectively (pooled from three simulations). (C) Scatter dot plot of key “points” of timelines from synchronized cell (a control condition’s plot is given for demonstrative purpose). Blue points are the starts of each simulated time line. Green points and red points represent the start and the end of HJURP association, respectively. The duration for each cell to be documented as “HJURP positive” cell is the distance between cognate green and red points, represented by the black bars in the schematics. All cells with their red points before the observational point (arrow, fixation and observation), and all cells with their green points after the observational point, will not be documented as HJURP-positive cells. The percentage of observed HJURP-positive cells (obs + %) can then be calculated based on these criteria. See Materials and methods for more details. (D, left) Simulated HJURP levels per centromere (mean \pm SD). Data were plotted using measurements from 10 random positions inside the HJURP-positive time window per simulation, three simulations in total. (right) Simulated percentages of HJURP-positive cells in control or perturbed populations with one round of thymidine synchronization (mean \pm SD). Percentage values were calculated from 40 independent simulations, 2,000 cells each. A.U., arbitrary unit. (E) Simulated loading curves of the number of CENP-A nucleosomes per centromere overlaid with experimental measurements shown in Fig. 2. For each condition, six representative simulation traces were plotted. For experimental data, mean \pm SD were shown. (F) Immunofluorescence detection of histone H2A.Z 48 h after transfection of indicated siRNAs (DNA - DAPI). Transfected cells were identified by cotransfected markers. Bar, 10 μ m. (G) Quantification showing the distribution of normalized H2A.Z integrated intensity per nucleus (mean \pm SD overlaid with scatterplots). Control ($n = 104$) and mDia2 siRNA ($n = 105$) cells from two independent experiments.



Video 1. **Side-by-side comparison of live cell imaging movies of a control cell and an mDia2 knockdown cell stably expressing YFP-CENP-A going through G1 phase.** Movies are on the same grayscale corresponding to Fig. 2 A (where image stills are pseudocolored in “jet” LUT). (left) A GAPDH siRNA cell as a control. (right) An mDia2 knockdown cell. Bar, 5 μm .



Video 2. **Another representative pair of cells (control and mDia2 knockdown) going through G1 after anaphase onset.** The movies are pseudocolored with the same “fire” LUT. (left) A GAPDH siRNA cell as a control. (right) An mDia2 knockdown cell. Bar, 5 μm .



Video 3. **A representative cell expressing YFP-CENP-A arrested in G1/S phase (in the presence of thymidine).** Cell was imaged every 20 min for 10 h.

Table S1. **Parameters used for numerical simulation of HJURP turnover**

Parameter	Value	Reference
k_{on} of an HJURP single molecule [HJURP]	$6 \times 10^8 \text{ M}^{-1} \text{ h}^{-1}$	Doherty et al., 2014
k_{off} of an HJURP single molecule	$2.33 \times 10^{-8} \text{ M}$	Doherty et al., 2014
Apparent duration of HJURP's association on centromeres	$\sim 1 \text{ h}^{-1}$	Doherty et al., 2014
Number of new CENP-A nucleosomes	3 h	Foltz et al., 2009
Timeline from thymidine release to fixation and observation of an early G1 cell	100	Bodor et al., 2014
	11 h	Foltz et al., 2009; McKinley and Cheeseman, 2014

References

- Bodor, D.L., J.F. Mata, M. Sergeev, A.F. David, K.J. Salimian, T. Panchenko, D.W. Cleveland, B.E. Black, J.V. Shah, and L.E. Jansen. 2014. The quantitative architecture of centromeric chromatin. *eLife*. 3:e02137. <http://dx.doi.org/10.7554/eLife.02137>
- Doherty, K., M. Meere, and P.T. Piiroinen. 2014. A mathematical model of CENP-A incorporation in mammalian centromeres. *Math. Biosci.* 249:27–43. <http://dx.doi.org/10.1016/j.mbs.2014.01.005>
- Foltz, D.R., L.E. Jansen, A.O. Bailey, J.R. Yates III, E.A. Bassett, S. Wood, B.E. Black, and D.W. Cleveland. 2009. Centromere-specific assembly of CENP-a nucleosomes is mediated by HJURP. *Cell*. 137:472–484. <http://dx.doi.org/10.1016/j.cell.2009.02.039>
- Lagana, A., J.F. Dorn, V. De Rop, A.M. Ladouceur, A.S. Maddox, and P.S. Maddox. 2010. A small GTPase molecular switch regulates epigenetic centromere maintenance by stabilizing newly incorporated CENP-A. *Nat. Cell Biol.* 12:1186–1193. <http://dx.doi.org/10.1038/ncb2129>
- McKinley, K.L., and I.M. Cheeseman. 2014. Polo-like kinase 1 licenses CENP-A deposition at centromeres. *Cell*. 158:397–411. <http://dx.doi.org/10.1016/j.cell.2014.06.016>
- Watson, J.V., S.H. Chambers, and P.J. Smith. 1987. A pragmatic approach to the analysis of DNA histograms with a definable G1 peak. *Cytometry*. 8:1–8. <http://dx.doi.org/10.1002/cyto.990080101>